Proceedings: The 11th International Seminar on Double Layer Capacitors,
Deerfield Beach, FL, U.S.A., December 3–5, 2001.

BIPOLAR SUPERCAPACITOR FOR 42 V APPLICATIONS

P. KURZWEIL
University of Applied Sciences, 92224 Amberg, Germany
H.-J. FISCHLE
Hydra Supercap GmbH, Sickingenstraße 71, 10553 Berlin, Germany

1 Technological outline

HYDRA are developing a novel bipolar multicell supercapacitor which combines the following advantages:

- operating voltages of up to 42 V,
- high specific energy (>2 Wh/kg) and power (>2 kW/kg),
- low internal resistance, long life and reliability,
- improved frequency response, self-discharge and temperature dependence of capacitance.

The development goals shall be achieved by a novel composite electrode [1] and electroactive materials [2] based on metal oxides, which show capacitances far above 1 F/cm^2 and 100 F/g.

The supercapacitor with improved performance is especially designed to cover peak loads required by applications such as

- short-term energy backup,
- pitch control in wind energy plants,
- automotive subsystems and future prospects (load-leveling, regenerative braking etc.).

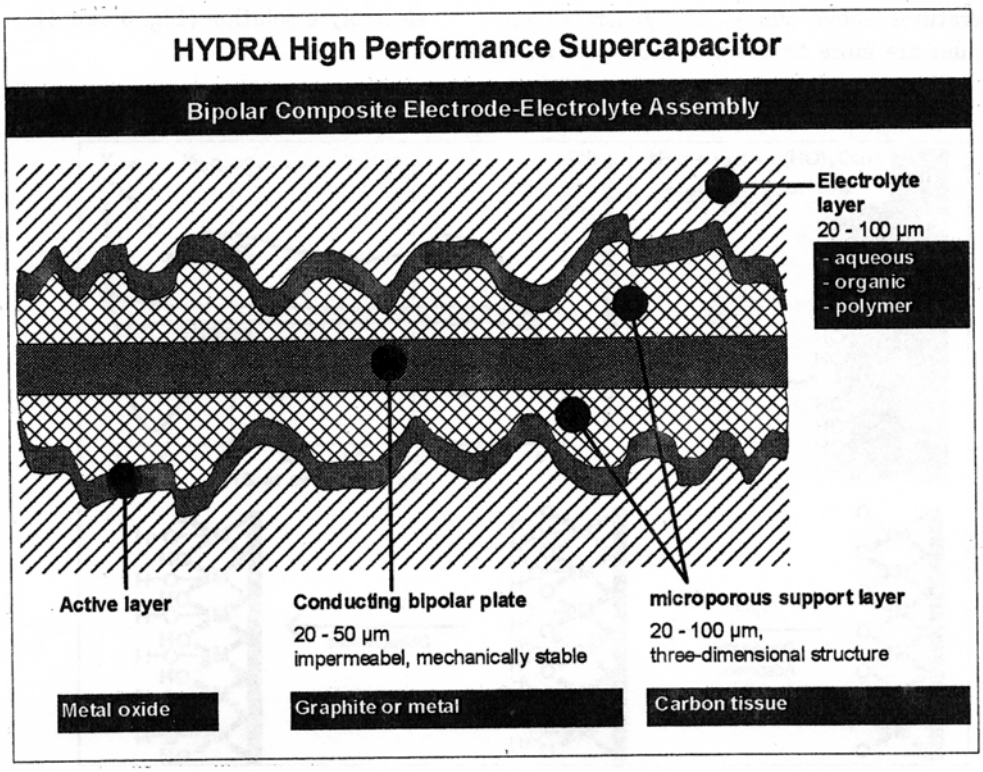

FIGURE 1: Porous electrode structure covered by an electroactive material.

A conductive material with a large surface forms a three-dimensional support structure for the electroactive layer (Fig. 1). As activated carbon materials are relatively expensive, the HYDRA electrode consists of low-priced commercial metal or carbon fibers, felts, papers or tissues. The electrocatalytic activity is obtained by a very thin layer of metal oxides [3, 4, 5]. The conducting bipolar plate consists of carbon or metal or a layer generated by a thermal spray process.

2 Electroactive materials

Precious metal oxides such als RuO_2 and IrO_2 have been known since the 1970s as highly active materials for dimensionally stable electrodes in alkali chloride electrolysis [6]. The observed redox activity [7] of these materials was used for supercapacitors later [8]. The pseudo capacitance of ruthenium oxide in aqueous solutions is caused by redox processes [5] (Figure 2).

$$RuO_x(OH)_y + z\ e^{\ominus} + z\ H^{\oplus} \rightleftharpoons RuO_{x-z}(OH)_{y+z}$$

Still in the early 1990s the active layer was produced by thermal spray pyrolysis of precursor solutions like $RuCl_3$ or H_2IrCl_6 directly onto the electrode support material. At decomposition temperatures above 500 °C, the generated metal oxides are more or less stoichiometric RuO_2 or IrO_2. They are most long-term stable, even at current densities of 1 A/cm^2. Their specific capacitances reach roughly 50 F/g in aqueous solutions.

The properties of platinium metal oxides depend dramatically on the details of their preparation and on the chemical composition of the active layer. Besides the electrical and ionic conductivity, morphological properties are decisive.

To increase capacitance, metal hydroxides were absorbed on carbon particles [9] and the water content of ruthenium oxide was found to be important.

To yield some hundred Farads per gram, our early approach [2] was to modify the rutile lattice by incorporating of defect atoms, which are able to bind water in an extended hydratation layer.

1. *Thermal decomposition* of precursor materials (such as $RuCl_3$) at about 300–350 °C together with alkali compounds generates an amorphous oxide lattice. The temperature should be in the phase transition of the chloridic preliminary stage and the hydrated oxide and can be determined from thermogravimetric curves. The residual content of bound chlorine and alkali ions in the rutile lattice can partially be exchanged by $H^{\oplus}$ and $OH^{\ominus}$ in the electrolyte solution (Fig. 3 and 4).

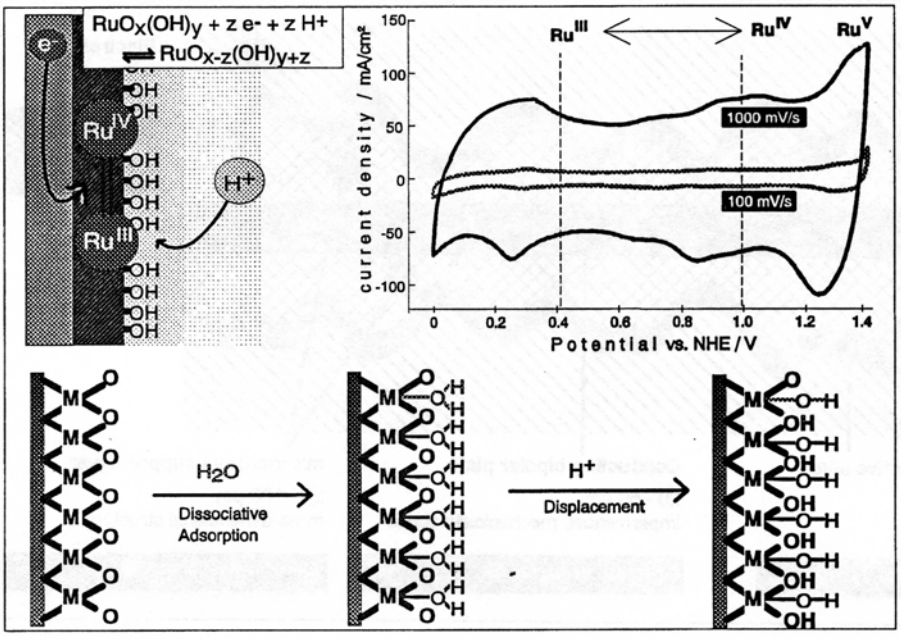

FIGURE 2: Cyclic voltammogram and mechanism of the redox capacitance of our RuO_2 electrode.

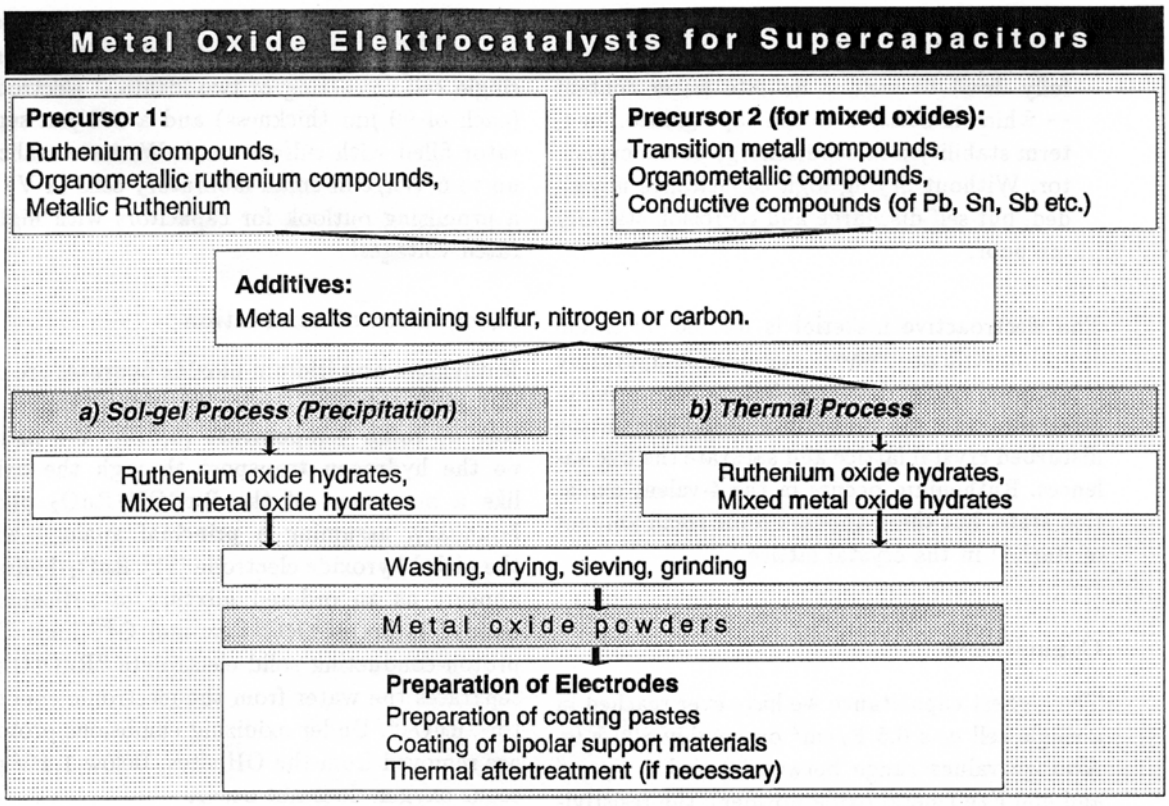

FIGURE 3: Synthesis of mixed metal oxide electrocatalysts for supercapacitors.

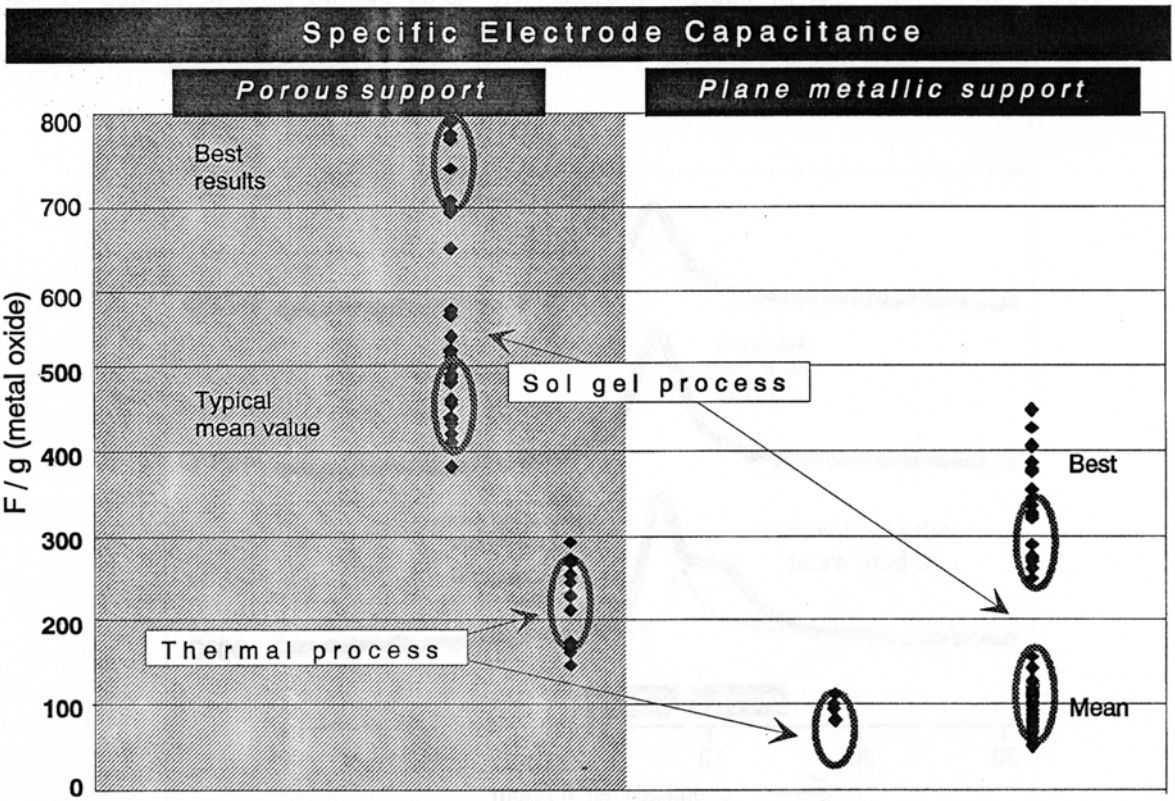

FIGURE 4: Specific capacitance of the metal oxide depending on the preparation method. Impedance measurements of single cells (at 0.1 Hz).

2. *Sol-gel process.* The precipitate of $RuCl_3$ in alkali hydroxide solutions is filtrated and carefully dried to yield a definite water content — which is decisive to the capacitance, long-term stability and selfdischarge of the capacitor. Without drying high capacitance is yielded, but self-discharge and corrosion stability are poor.

The electroactive material is formed by a non stoichiometric amorphous metal oxide-hydroxide ("hydrated oxide" $RuO_{2-x}(OH)_y$). Water molecules surround the ruthenium atoms within the disturbed crystal lattice and saturate the free valences. Ruthenium occurs in the 4-valent oxidation state, but there appears some small amount of Ru(III) in the crystal lattice.

Capacitance

The highest capacitance we have ever reached in a single cell was 6.5 F/cm^2 or roughly 800 F/g. Average values range between 2 and 4 F/cm^2 and 450 F/g (metal oxide powder); the resistivity of a single cell is $<0.1\ \Omega$ cm.
We consider 8 F/cm^2 to be the upper limit which can be reached with platinum metal oxides on three-dimensional electrode supports. This corresponds to an energy density of 20 Wh/ℓ for a single cell consisting of two identical electrodes (each of 90 μm thickness) and a 100 μm separator filled with sulfuric acid. We have realized up to 6 Wh/ℓ in small laboratory cells (1 V) — a promising outlook for capacitors with higher rated voltages!

Mechanism of conduction

Ruthenium and iridium dioxide hydrates are mixed electronic and ionic ("protonic") conductors at room temperature [5, 10]. We imagine the hydrogen transport through the oxide like a movement of the $RuOOH/RuO_2$ phase boundary, assuming a principal analogy with the nickel hyroxide electrode [11]. RuO_2-hydrate appears as an ordered mixture of ruthenium-bonded layers of $OH^{\ominus}$ ions and $O^{2\ominus}$ ions. The proton-conducting solid electrolyte "RuO(OH)" separates the water from the electronic conductor "RuO_2". Under oxidizing conditions protons are removed from the OH sites. Below 1.4 V gaseous oxygen does not occur.
Our 300 MHz ^{1}H-MAS-NMR investigation [10] hints at two sorts of protons in RuO_2-hydrate.

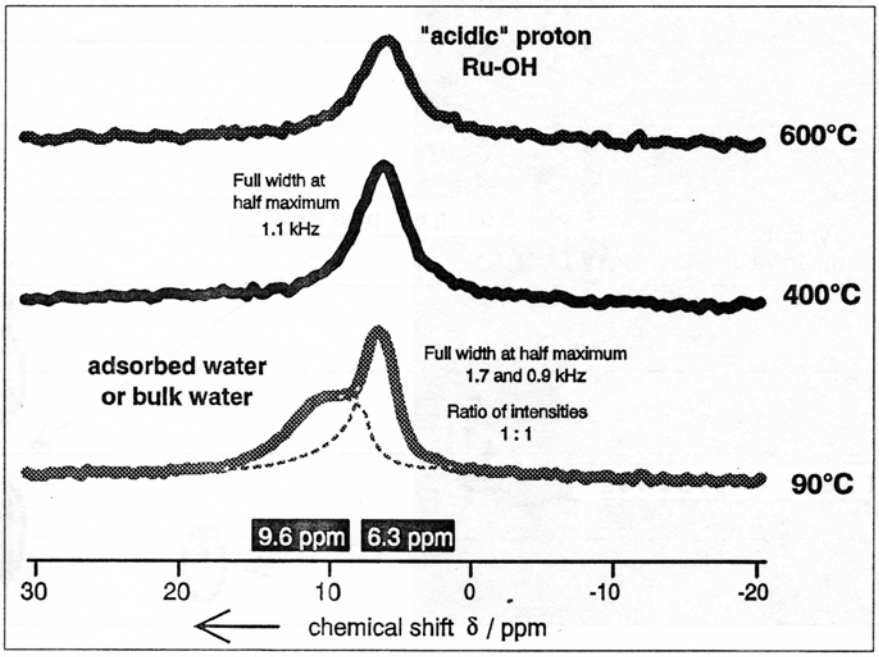

FIGURE 5: ^{1}H-MAS-solid state NMR-spectrum of ruthenium dioxide-hydrate dryed at different temperatures.

- Protons of absorbed or bulk water (9.6 ppm), which disappears at elevated temperatures (just as capacitance does).
- Protons of OH-groups, which are still observable in 600 °C powders.

At elevated temperatures adjacent OH-groups condensate to form Ru-O-Ru–bonds, which are not able to bind protons — and consequently specific capacitance falls.
The OH-groups should be the more acidic the smaller their number is, if some analogy with silicagels is assumed. Without water present considerable proton mobility and Ru^{IV} oxidation cannot happen. Water seems to be a carrier for the proton in RuO_2 (vehicle mechanism). Probably the autoprotolysis of water plays a role to generate and transport easily mobile protons and to stabilize the Ru^{III} state.

$$[\mathrm{Ru}]{\leftarrow}(\mathrm{H_2O}) \rightleftharpoons [\mathrm{Ru}]{-}\mathrm{OH}^{\ominus} + \mathrm{H}^{\oplus}$$

We have not found any signals of protons near paramagnetic centers, so there is *no evidence for Ru-H–bonds* in the powder. As stressed above, protons form OH-groups at oxide sites in the rutile lattice.

3 Performance Data

The **short-circuit power** during the discharge of a 15 V/100 F supercapacitor exceeds 30 kW or 6 kW/kg in the 500 micro second range (Fig. 6). Current, voltage and power were recorded using an oscilloscope. The internal resistance of the capacitor equals 2.5 Ω (at 0.4 s); total mass is 5 kg, total volume 4,3 ℓ.

Frequency response

The impedance spectrum (Fig. 7) shows that the capacitive properties of the supercapacitor are definitely guaranteed below 1000 Hz. The decline of capacitance towards high frequencies is less severe than with capacitors based on carbon materials.
The capacitance was calculated based on the admittance for every frequency.

$$C(\omega) = \frac{\mathrm{Im}\,\underline{Y}}{\omega} = \frac{-\mathrm{Im}\,\underline{Z}}{\omega\,|\underline{Z}|^2}$$
$$|\underline{Z}| = \sqrt{(\mathrm{Re}\,\underline{Z})^2 + (\mathrm{Im}\,\underline{Z})^2}$$

$\omega = 2\pi f$ is the circular frequency. $\mathrm{Re}\,\underline{Z}$ and $\mathrm{Im}\,\underline{Z}$ are ohmic resistance and reactance respecticely.

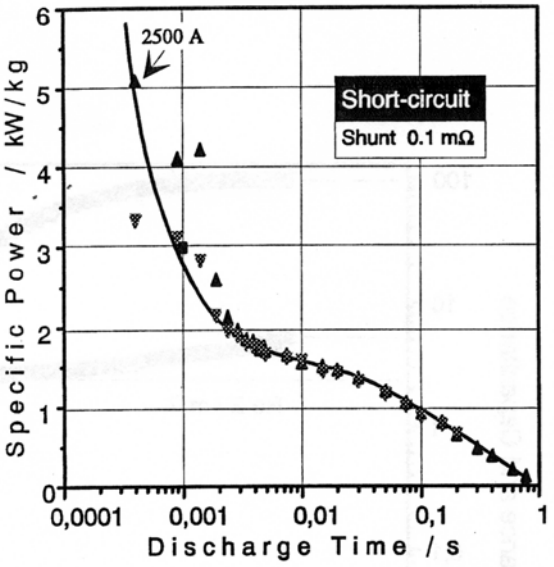

FIGURE 6: Short-circuit characteristic of a 15 V/100 F supercapacitor.

The capacitance reaches its maximum below 1 Hz, when there is time enough for slow electrode reactions to occur in the pores of the electrode material. At high frequencies it is primarily the "outer" electrode surface which is charged and discharged [5]. Accordingly, there is a strong decline of capacitance when there is not enough time for the concentration wave to penetrate deeply into the pores. Above 5000 Hz inductive behavior plays an increasingly important role.
Capacitance and voltammetric charge depend on mass and porosity of the coating. Thick porous layers reduce the slope of the low-frequency straight line and increase the high-frequency "charge-transfer" quartercircle (Figure 8). This "pore diffusion" behaviour is a critical quantity that has to be optimized by the pore structure and thickness of the electrode.

Temperature dependence

The temperature dependent capacitance shows an exponential decline with an apparent activation energy of 3.4 kJ/mol (Fig. 10). This is typical for the rapid electrokinetic processes occuring at the electrode/electrolyte interface. The capacitor can be operated between −40 and +120 °C, if sulfuric acid or potassium hydroxide is used.

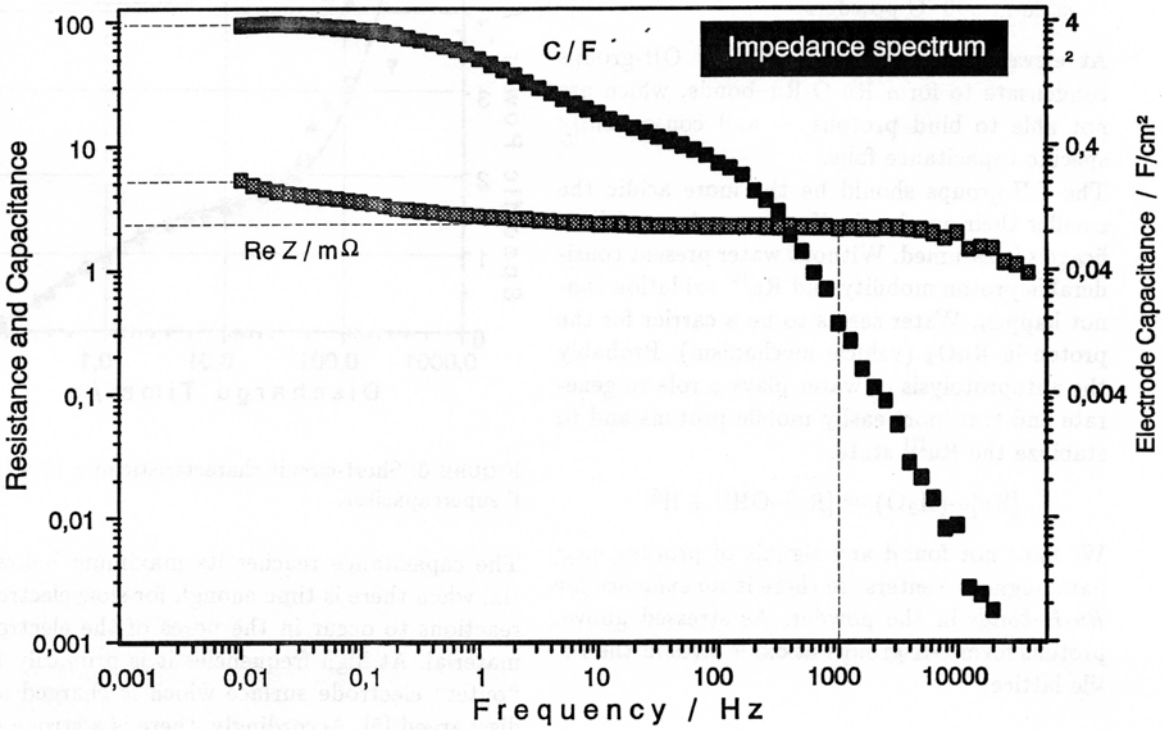

FIGURE 7: Frequency response of ohmic resistance and capacitance of a 15 V/100 F capacitor.

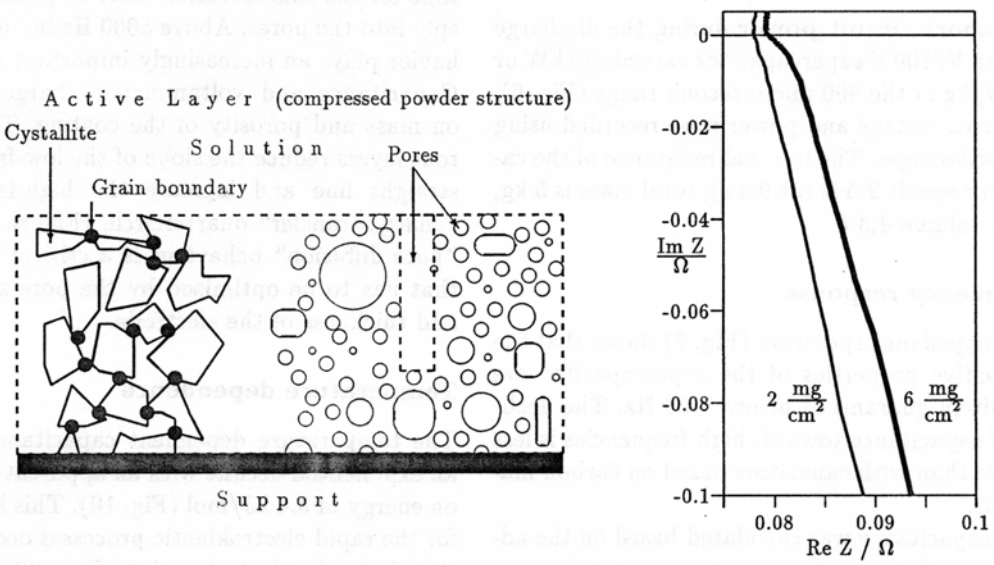

FIGURE 8: The effect of the morphology of oxidic layers on the impedance spectrum (electrodes with different active mass). Note the different scaling of real and imaginary axis for the purpose of illustration.

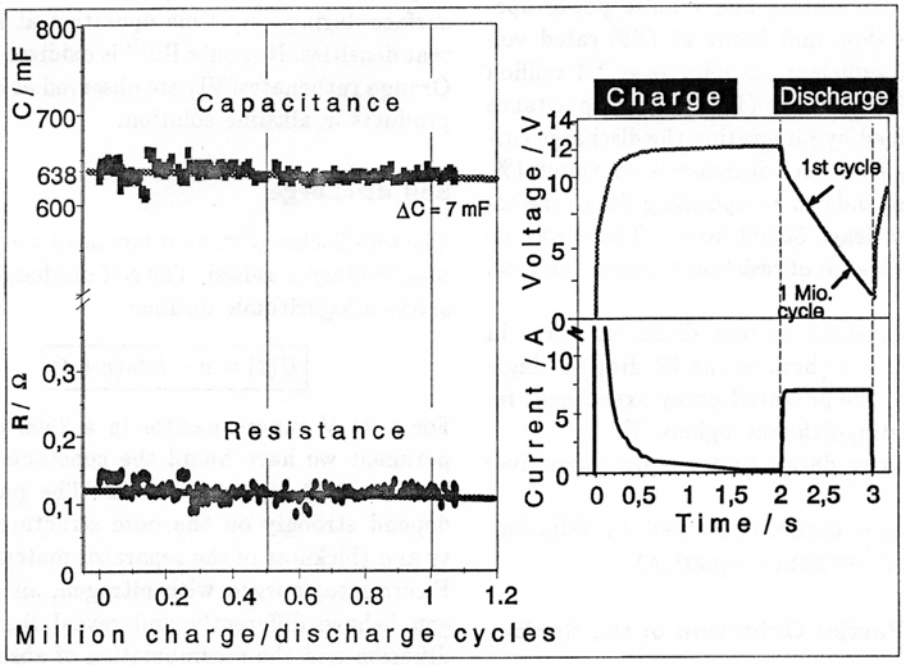

FIGURE 9: Life test of a 0.64 F metal oxide supercapacitor: Transients of voltage and current during 1.2 million cycles (at 12 V, 210 mA/cm^2. Peak charging current 40 A).

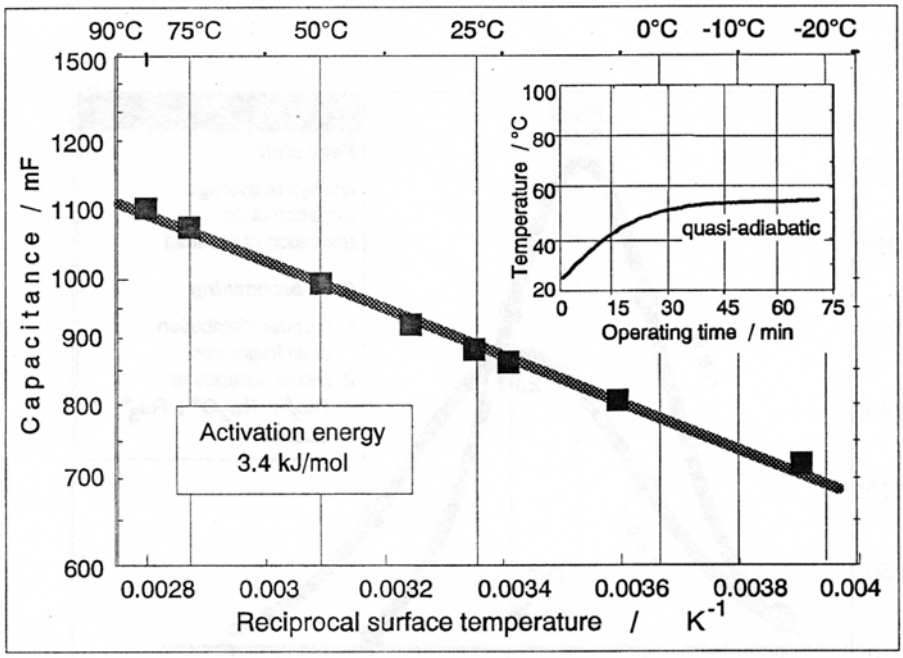

FIGURE 10: Temperature dependence of capacitance of a 24 V/1 F metal oxide supercapacitor following the Arrhenius law (Operating voltage 12 V). Inner picture: Surface temperature profile of the wrapped-in capacitor at room temperature without convection.

Life Test

Accelerated life testing under pulse power operation for a thousand hours at 50% rated voltage proved sufficient stability over 1.1 million charge/discharge cycles (Figure 9). Capacitance was determined by integrating the discharge curve: $C = \frac{1}{\Delta U} \int I\, dt$. Its decrease is by about 1%, which corresponds to an operating life of the capacitor of at least 50000 hours. There was no significant increase of resistance during the total test period.

While the constant current discharge curve in the Figure shows (besides the IR drop) a single linear region, the potential decay experiment reveals two distinguishable regions [7]:

a) a short-term decay (not simply capacitive) and

b) a long-term decay, controlled by diffusion: $I \sim \sqrt{D/t}$ (COTTRELL's equation).

Aging by Partial Oxidation of the Surface

In the SIMS spectra of new and used (after life test) RuO_2 electrodes we compared the intensities of the $RuO_n^{\ominus}$ fragments and found a shift of nearly half of an oxidation state (Figure 11). This result should only be conceived qualitatively, but it reveals the partial oxidation of the surface during long time operation at high current densities. Not only Ru^{III} is oxidized to Ru^{IV}. Orange ruthenates(VI) are observed as corrosion products in alkaline solution.

Self discharge

The self-discharge current increases when the applied voltage is raised. The self-discharge voltage shows a logarithmic decline:

$$\boxed{U(t) = a - b \ln(c + t)}$$

For a 24 V supercapacitor in a 2000 hours experiment we have found the constants $a = 4.2$ V, $b = 0.32$ V, $c = 8.4$ hrs. The parameters depend strongly on the pore structure, porosity and thickness of the separator materials used. Electrolytes purged with nitrogen, air and oxygen behave differently and reveal that oxygen diffusion and the recombination of absorbed hydrogen and oxygen play a major role.

$$^1/_2 O_{2\,(\text{electrolyte})} + 2\,H_{\text{electrode}} \rightleftharpoons H_2O$$

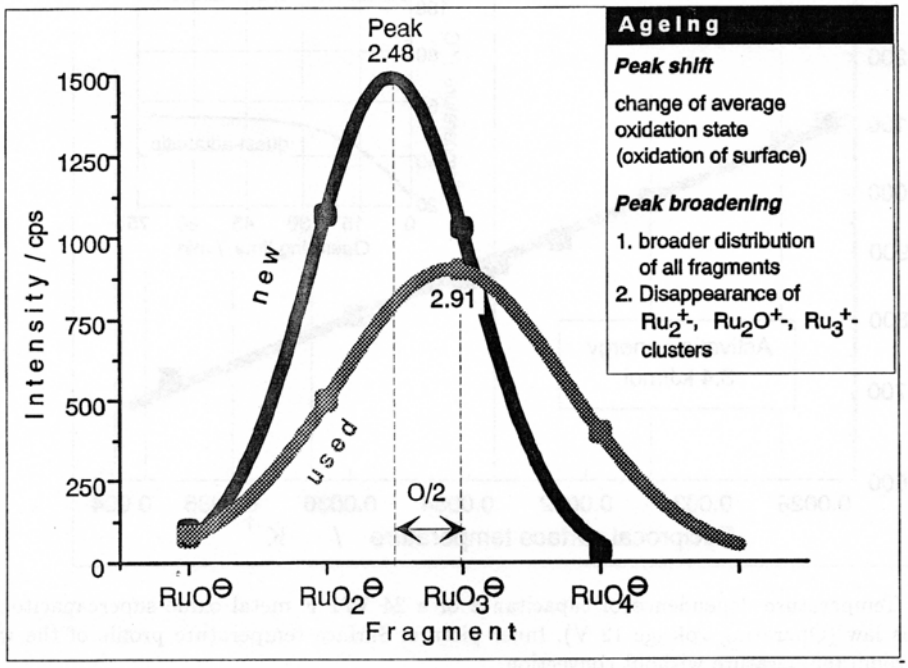

FIGURE 11: Secondary Ion Mass Spectroscopy (SIMS) of new and aged metal oxide electrodes: Analysis of RuO_n fragment ions.

With respect to the hydrogen sorption it is not astonishing that cyclic voltammograms of supercapacitor single cells are very similar to those measured at RuO_2 electrodes versus the reversible hydrogen electrode (except the location of the reduction peaks).

References

[1] Double-layer capacitor, DE 197 04 584 C2 (1999).

[2] Long time stable electrode, EP 0 622 815 B1 (1996), DE 43 13 474 A1 (1994).

[3] *German patent* DE 196 40 926 C1 (1998).

[4] (a) P. KURZWEIL, G. DIETRICH, Double-layer capacitors for energy storage devices in space applications, *Proc. 2nd Int. Seminar on Double Layer Capacitors and Similar Energy Storage Devices*, Deerfield Beach, Florida (1992).
(b) P. KURZWEIL, O. SCHMID, High performance metal oxide supercapacitors, *Proc. 6th Int. Seminar on Double Layer Capacitors*, Deerfield Beach, Florida, December 9–11 (1996).
(c) P. KURZWEIL, O. SCHMID, A. LÖFFLER, Metal oxide supercapacitor for automotive aplications, *Proc. 7th Int. Seminar on Double Layer Capacitors*, Deerfield Beach, Florida, December 8–10 (1997).

[5] (a) S. TRASATTI, P. KURZWEIL, Electrochemical supercapacitors as versatile energy stores. Potential use for platinum metals, *Platin. Metal. Rev.* **38** (1994) 46–56.
(b) S. TRASATTI, *Electrochim. Acta* **36** (1991) 225.
(c) A. DAGHETTI, G. LODI, S. TRASATTI, *Mater. Chem. Phys.* 8 (1983) 1.

[6] (a) S. TRASATTI, Electrodes of conductive metallic oxides, Part A, pp. 332ff, Elsevier, Amsterdam (1980).
(b) H. B. BEER, *J. Electrochem. Soc.* **127** (1980) 303C.

[7] (a) S. TRASATTI, G. BUZZANCA, *J. Electroanal. Chem.* **29** (1971) 1.
(b) K. DOBLHOFER, M. METIKOS, Z. OGUMI, H. GERISCHER, Electrochemical oxidation and reduction of the RuO_2/Ti electrode surface, *Ber. Bunsenges. Phys. Chem.* **82**, 1946–1050 (1978).

[8] Among others: (a) R. D. CRAIG, *Canadian patent* 1 196 683 (1985).
(b) PINNACLE „Ultracapacitor" (1989–1994); *IEEE Trans. Magn.* **25** (1989) 102.
(c) J. MCHARDY, *Proc. 22nd Intersoc. Energy Convers. Eng. Conf.* (1987) Vol 1., 306.
(c) B. E. CONWAY, *J. Electrochem. Soc.* **138** (1991) 1539.
(d) GINER (1990; S. SARANGAPANI *et. al.* US 5 136 474 (1992)).
(e) DORNIER (DaimlerChrysler Group, 1990–1997 [4]).
(f) Army Research Laboratory: J. P ZHENG, T. R. JOW, *J. Electrochem. Soc.* **142** (1995) L6 and 2699.
(g) I. D. RAISTRICK, in: Electrochemistry of Semiconductors and Electronics Processes and Devices (eds.: J. McHardy, F. Ludwig), Noyes, Park Ridge NJ (1992) 297.

[9] MALASPINA, US 5 079 674 (1992).

[10] P. KURZWEIL, O. SCHMID, Low temperature proton conducting metal oxide supercapacitor, *Meeting Abstracts*, The Electrochemical Society Fall Meeting, San Antonio, Texas, October 6–11 (1996) 825.

[11] R. A. HUGGINS, H. PRINZ, M. WOHLFAHRT-MEHRENS, L. JÖRRISSEN, W. WITSCHEL, Proton insertion reactions in layered transition metal oxides, *Solid state ionics*, **70/71**, 417–424 (1994).